

Ultra-pure single wall carbon nanotube fibers continuously spun without promoter

Catharina Paukner, Krzysztof K.K. Koziol*

Department of Materials Science and Metallurgy, University of Cambridge, 27 Charles Babbage Road, CB3 0FS Cambridge UK.

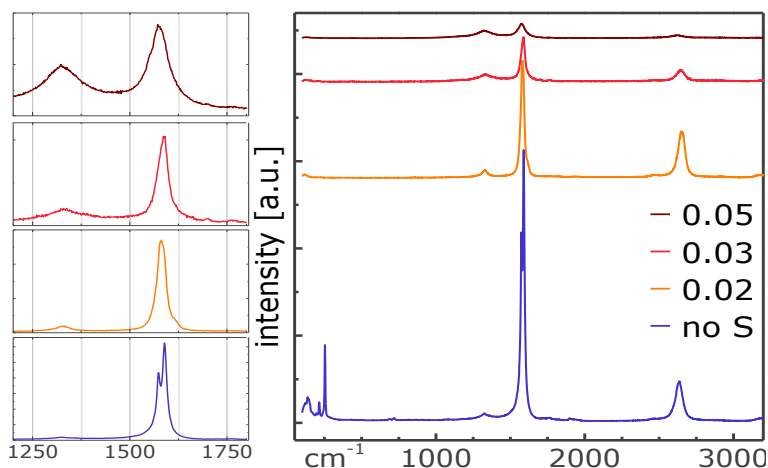


Table S1. Raman D/G and D/2D peak intensity ratios according to the amount of sulphur compound in the feedstock. S/C ratio

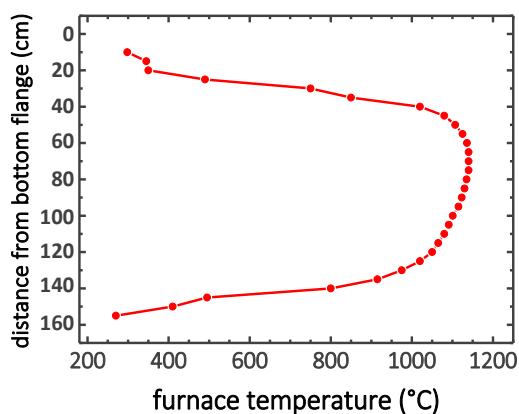
feedstock S/C	Raman D/G	Raman D/2D
0.05	0.56	2.22
0.03	0.19	0.67
0.02	0.07	0.18
no S	0.05	0.21

Figure S1. Raman spectra of CNT fibre generated from toluene and ferrocene (figure 1) with and without thiophene normalised to the D peak (D=1), offset along the y axis with zoom in on the D and G peak region.

Table S2. Injection temperature as a function of injection depth and carrier gas flow.

Inj T (°C)	Inj. depth (cm)	hydrogen flow (mL/min)
360	15	1200
330	15	1000
316	15	900
300	10	1500
250	10	1350
238	10	1200
234	10	1050
228	10	1000

Figure S2. Furnace temperature profile measured in an Ar flow of 1.2 L/min in the centre of the tube.



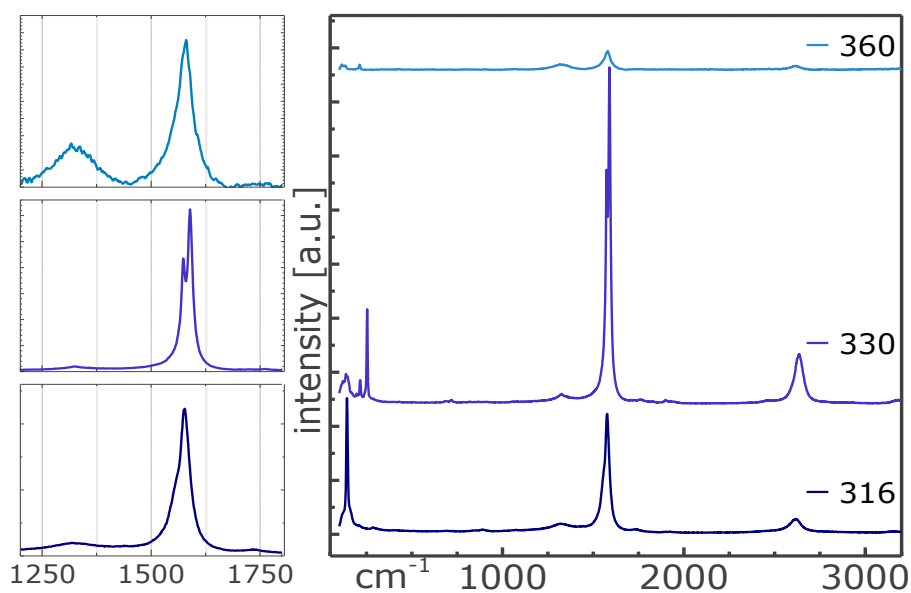


Figure S3. Raman spectra of CNT fibre sample from 15 cm injection depth normalised to the D peak ($D=1$) and listed according to their injection temperature offset along the y axis with zoom in on the D and G peak region.

Table S3. Overview of sample values according to injection temperatures.

Inj. depth (cm)	Inj T (°C)	Fe/C feedstock	Fe residue (%)	D/G	D/2D	RBM ω ($I_{\text{RBM}}/I_{\text{G}}$)
15	360	0.0007	2.6	0.47	1.33	114.5 (0.52); 211.9 (0.46); 132.3 (0.43)
15	330	0.002	7.4	0.03	0.21	254.0 (0.28); 119.8 (0.07); 137.6 (0.09); 196.0 (0.03); 215.4 (0.07)
15	316	0.002	0.3	0.09	0.70	142.9 (1.13); 211.9 (0.08); 285.4 (0.06)
10	300	0.031	15	0.03	0.11	150.0 (0.69); 194.2 (0.14); 217.1 (0.09)
10	250	0.034	29	0.10	0.38	218.9 (0.26); 199.5 (0.12); 254.0 (0.08)
10	228	0.028	15	0.52	4.06	201.0 (0.39); 208.0 (0.35)

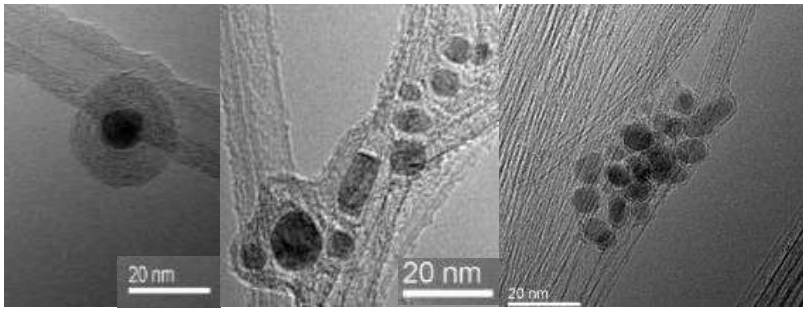


Figure S4. Catalyst poisoning in various CNT fiber samples: a) multiple graphene layers encapsulating a round catalyst particle, b) metal particles in various shapes, cluster created by carbon layering and c) agglomerate of oval catalyst particles.

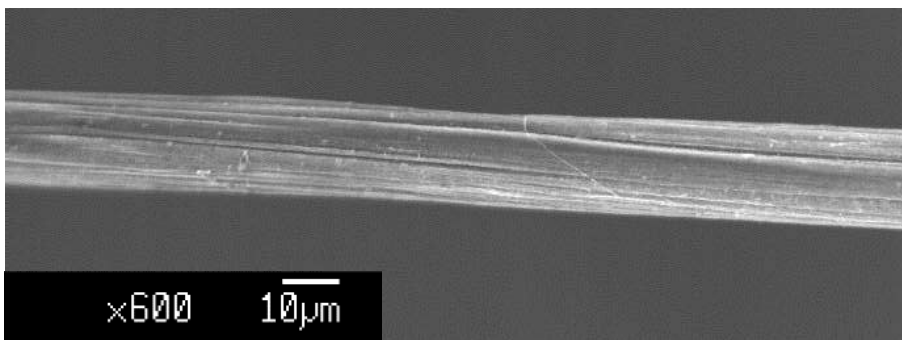


Figure S5. Low magnification image of CNT fibre sample 10_3.

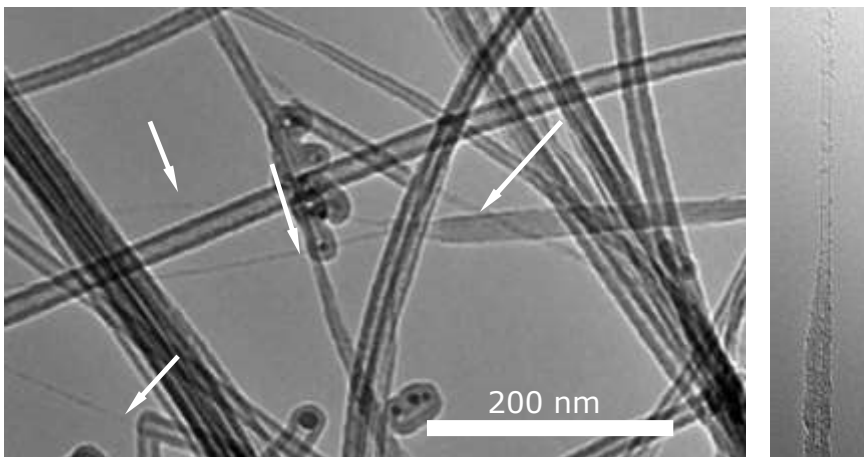


Figure S6. TEM image of single wall adjuncts to MWNTs of varying diameters (indicated by arrows) providing an explanation for RBMs observed in Raman spectroscopy.

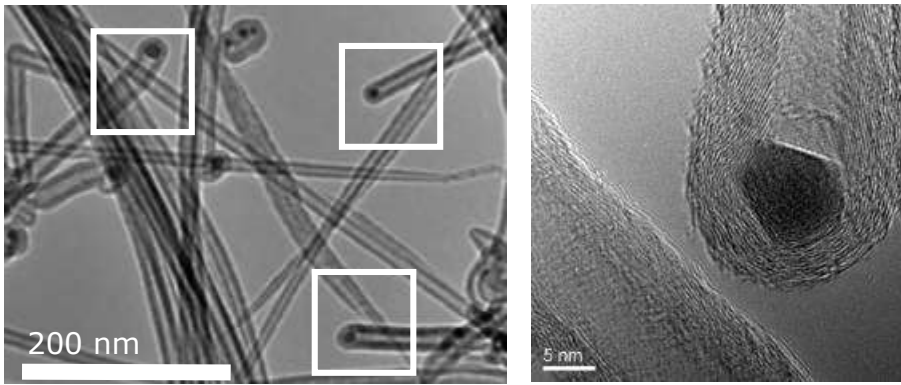


Figure S7. Herring bone structured MWNT with catalyst particle confirming assumption of epitaxial growth.